[EA]Facies Modeling of a Giant Carbonate Gas Reservoir Severely Affected by Secondary Overprint An Example from the Khuff Gas Reservoir, Awali Field, Bahrain*

Jayanta Bardalaye[1], Michael Dowen[1], and Lana Al Hashemi[1]

Search and Discovery Article #20458 (2019)**
Posted March 25, 2019

*Adapted from extended abstract prepared in conjunction with poster presentation given at GEO 2018 13th Middle East Geosciences Conference and Exhibition, Manama, Bahrain, March 5-8, 2018
**Datapages © 2019 Serial rights given by author. For all other rights contact author directly. DOI:10.1306/20458Bardalaye2019

[1]Tatweer Petroleum, Awali, Bahrain (Jayanta_Bardalaye@tatweerpetroleum.com)

Abstract

The Awali Field in Bahrain is the first hydrocarbon discovery in the Arabian Gulf region in the year 1932. It has oil and gas accumulations in different stratigraphic intervals. The Permian Khuff carbonates hosts a giant gas accumulation that meets the energy requirements of the Kingdom of Bahrain.

Lithologically, the Khuff is dominantly dolomite with minor limestone, anhydrite, and occasional thin shale intervals. Core coverage is limited and mostly concentrated in the reservoir zones. Studies on the limited available cores suggest presence of at least six diagenetic events. This has completely obliterated the original fabrics. Identifying facies from well logs with poor core control is therefore an extremely daunting task. Presence of dolomite and anhydrite as part of both the matrix as well as cement further compounds the problem.

Different vintages of open-hole well logs are available in most of the wells. Mineral volume curves generated from elemental spectroscopy logging in the wells drilled in the recent past have been used to define a practical and usable facies classification. This input was used in Petrel to generate a 3D facies model. The facies-controlled porosity model prepared subsequently provides a realistic picture of the subsurface reservoir architecture.

Introduction

The Bahrain Field (Figure 1) is an asymmetrical anticline trending in the north-south direction. The field was discovered in 1932. The field is multi-stack carbonate and sandstone reservoirs most of them oil bearing (Kumar et al, 2003). The Permian Khuff dry gas reservoir was discovered in 1948. Commercial development of the reservoir started in 1969 by drilling 2 wells to meet the energy requirements of the rapidly industrializing Kingdom (Janahi et al, 1985). As on date, 49 wells have been drilled in the reservoir in phases.

Khuff Geology

Structure: The Awali structure is an elliptical, asymmetrical dome elongated in the north-south direction (Figure 2). The western flank has a higher dip than the eastern flank. A north-south trending graben is located at the crest of the structure. The graben is asymmetrical with the large, west dipping faults (maximum throws of 200-300 ft) on the eastern side. Faults on the western side of the graben generally have throws less than 100 ft.

Stratigraphy: The Permian Khuff reservoir is predominantly dolomite, but it contains lesser amounts of limestone, dolomitic limestone, and anhydrite. Occasional thin shale intervals are also seen in some wells. The thickness thickens from about 1900 ft on the crest of the structure to more than 2150 ft off-structure The Khuff is traditionally divided into four units: the K0, K1, K2, and K3 (from top to bottom). The tops of the K1 and K2 are placed at the top of the two main porous zones. Matrix porosity is restricted to parts of the K0 to K2 interval, with the best reservoir quality in the K2. K3 is tight with some fracture porosity developed close to the major faults.

Sequence stratigraphic analysis of the Khuff reservoir was carried out in 2002 that helped in identifying transgressive-regressive units within the Khuff (unpublished-CGG and BAPCO, 2001). However, the sequence model developed for the Khuff was highly provisional, due to the limited core data and some lithological characteristics. The low clay content of the Khuff makes it difficult to accurately position maximum flooding surfaces (MFS), and there is insufficient core to identify the log signature associated with the most distal facies. It is easier to identify sequence boundaries (SB). In all 22 sub-units (Figure 3) were identified within the Khuff and the same scheme was extrapolated to the wells drilled subsequently. The sequence boundaries are generally identified by an overlying basin-ward shift of facies belts. The two best candidates for 'time horizons' are the top of unit 5 (K1_5_SB) and the pair of anhydrite beds at the base of unit 6c (Figure 9). Both horizons correspond to important sequence boundaries. The upper horizon, which is perhaps the most important marker in the field, separates different depositional systems. The base of the anhydritic bed near the top of K3 is another probable 'time horizon'. In the modelling process, each sequence stratigraphic unit was considered as a separate zone.

Diagenesis: Core coverage is limited and mostly concentrated in the reservoir zones. Studies on the limited available cores suggest presence of at least six diagenetic events (Figure 4). The sequence began as compaction of limestone components subsequently dissolved. Dolomite crystals nucleated throughout the host. The replacement process completely obliterated the original fabrics. This process may be syn-dolomitization controlled by rates of calcite / aragonite dissolution and dolomite growth. Subsequent rare allochem dissolution followed. Later stage clear dolomite rhombs precipitated within pore spaces. Possible changes in environmental conditions led to precipitation of evaporite minerals, like anhydrite cement within pore spaces (Figure 5). Minor amounts of pyrite and siderite precipitated impinging on dolomite crystals. The sequence of diagenetic events is interpreted to be:

1. Compaction.
2. Extensive dolomite replacement of pre-existing limestones.
3. Dissolution of skeletal grains resulting in moldic/intraparticle pores.
4. Late stage dolomite precipitation.
5. Precipitation of evaporate mineral anhydrite.

6. Pyrite and siderite.

Petrophysical Model

Most wells only have conventional logs (Resistivity, Density or Sonic, Neutron, GR). However, some wells do have a full suite of open-hole logs across the Khuff reservoir intervals which included a Lateral Resistivity, Density with Photo Electric curve, Neutron, Sonic, GR, and an Induced Gamma Ray Spectroscopy tool. Due to the completeness of the data set in these wells, they were chosen as base wells for development of the Petrophysical Model.

Mineral Model Incorporating ECS

Senergy's Integrated Petrophysics (IP ™) software was used for the petrophysical analysis. The inputs to the Mineral Solver module were those usually obtained with a regular Resistivity-Porosity tool combination, as well as mineral dry weight fractions calculated from the Induced Gamma Ray Spectroscopy tool's elemental data. The anhydrite, clay, quartz, and siderite mineral fractions were used with low uncertainties to control the non-carbonate mineral volumes. The dolomite and calcite volumes were predominantly resolved by the Density – Neutron – Photo Electric curves. The resulting interpretation is shown in Figure 6. Crucially the major minerals - calcite, anhydrite, and dolomite - appeared to be in reasonable distribution and matched core and lithology from mud logs in offset wells. In one well, the upper part of K1 dolomite-calcite interval (which is the most permeable part in K1) exhibited the highest abundance of clay as calculated by the IGRS. Additionally, this interval contained siderite and significant titanium signature, which is usually associated with smectite. However, examination of the lithology across the interval from mud logs and cores from offset wells do not show presence of any clay in the interval. Clay, being an insignificant occurrence over the entire Khuff interval, the high clay reading was therefore attributed to barite invasion during drilling and was not used in the final mineral model.

Mineral Model Excluding ECS

Since most wells only had conventional logs (Resistivity, Density or Sonic, Neutron, GR) a simpler model was used. A model was developed in which the ECS was not utilized. Due to the similar grain densities of the carbonates and anhydrite, the anhydrite volume calculation was only invoked when the bulk formation density was 2.88 gm/cc or higher. Above this value the mineral was assumed to be 100% anhydrite. The mineral compositions for this model is shown in Figure 7. This model was used for all other wells for which ECS data was not available.

Facies Classification

Severe diagenesis has totally obliterated the primary rock fabric. So, a conventional facies classification cannot be used. The mineral volume curves generated from the petrophysical model were imported into Petrel and used as inputs to classify facies to be used in the geomodelling process. Just as lithology is interpreted in a mud log depending on the proportion of the various lithologies seen in cuttings, similarly the proportion of minerals in a particular depth interval was used to interpret the facies using the following cut-off:

Lithofacies	Mineral Proportion (%)
Dolomite	>= 80% Dolomite
Porous Dolomite	>= 80% Dolomite, Porosity >= 3%
Limestone	>= 80% Calcite
Porous Limestone	>= 80% Calcite, Porosity >= 3%
Anhydrite	>= 80% Anhydrite
Calcitic Dolomite	15% - <50% Calcite, >50% - 75% Dolomite
Porous Calcitic Dolomite	15% - <50% Calcite, >50% - 75% Dolomite, Porosity >= 3%
Dolomitic Limestone	15% - <50% Dolomite, >50% - 75% Calcite
Porous Dolomitic Limestone	15% - <50% Dolomite, >50% - 75% Calcite, Porosity >= 3%

The different facies codes are shown in Figure 8. One well with ECS was used as a standard well to identify the different lithofacies and create a facies log. Then a supervised classification was done for the other wells using the facies log from the standard well as the training log (Figure 9). In the final facies distribution, dolomitic limestone and porous dolomitic limestone (facies code 3 and 4) were not picked up in the facies logs.

Facies Modelling

Each identified sequence stratigraphic systems tract was modelled as a separate zone during the “Make Zone” process. The final zone distribution was 5 zones each in K0 and K1, 4 zones in K2, and 8 zones in K3. The layer thickness was set to capture the anhydrite beds that can act as vertical permeability barriers, especially in the bottom part of K0 and K1 and top part of K3. The generated lithofacies logs were then upscaled and made ready for the data analysis process.

Data Analysis: Vertical facies proportions (Figure 10) were investigated for each of the 22 zones to match the vertical facies distribution observed in cored wells and mud logs. In most of the zones, the upscaled facies logs have captured the vertical facies distribution very well. In few wells minor adjustments had to be made to match the vertical facies distribution. Similarly, the thickness histograms were analyzed to ensure that the cell thicknesses were at adequate resolution to capture the heterogeneity. Facies probability analysis was not attempted as there is no secondary attribute to work out a relationship with.

Variogram analysis were carried out for each facies per zone (Figure 11). Wherever possible, the major and minor ranges were determined based on this analysis. However, this was not possible for all the facies in all the zones. Regional stratigraphic understanding and log correlations were used to determine the ranges and direction in such cases.

Facies Modelling: Sequential Indicator Simulation (SIS) was used to model the facies in 3D space. The vertical facies proportions and variograms were used from the data analysis process. Facies fractions were manually edited to match global distribution where required. This was done for each facies per zone. Facies histograms were examined to ensure proper distribution matching the input data (Figure 12).

The resultant facies model is shown in Figure 13 (sectional view).

Porosity Modelling

The corrected porosity logs from the petrophysical model were imported into Petrel. The logs were then upscaled. The cell thicknesses used for the facies log upscaling captured the vertical porosity distribution also in a good way (Figure 14). Facies-controlled data analysis was then carried out for each facies per zone. First, required transformations were applied to remove any trend in the data. Then variograms were analyzed to determine the azimuth and ranges of the major and minor directions, where possible. As with the facies modelling, regional understanding was used to determine the variogram ranges where data analysis could not provide reliable results.

Sequential Gaussian Simulation (SGS) was applied to model the porosity in 3D space. The facies model was used as a constraint to populate the porosity. Transformations from the data analysis process were used to remove any trend in the populated 3D volume. The facies-controlled 3D porosity model provides a realistic picture of the subsurface reservoir architecture (Figure 15).

Conclusions

The Khuff carbonate reservoir in the Awali Field has been severely affected by secondary overprint. At least 6 diagenetic events have obliterated the primary rock fabric. Mineral volume curves generated from well logs have been used to generate a workable lithofacies scheme. 3D facies modelling using such facies logs has given a reasonable picture of the subsurface facies distribution. The porosity model created using the facies model as a constraint is a good representation of the reservoir architecture.

Acknowledgement

The authors are thankful to the management of Tatweer Petroleum for permission to publish this paper. Special thanks to Yahya Al-Ansari, Subsurface Manager, Najla Nedham, Head-Deep RMT, and Ali Al-Muftah, Head-Studies Team for their constant encouragement and support. The authors are also thankful to all their colleagues for their valuable critiques and suggestions.

Selected References

Banoco, 1965. BRT Report, by the Exploration and Development Department (Unpublished).

Banoco, 1980. A Comprehensive Review of the Bahrain Field (Unpublished).

CGG and BAPCO, 2001. Khuff and Unayzah Reservoir Characterization Study, Final Report from Phase I of Awali Field Reservoir Characterization Study (Unpublished).

CGG – BAPCO Team, August 2002, Awali Field Study (Unpublished).

Janahi, I.A., and B.A. Dakessian, 1985, Development of the Khuff Gas Reservoir, Bahrain Field: Middle East Oil Technical Conference and Exhibition, 11-14 March, Bahrain, SPE 13679, 25 p. doi.org/10.2118/13679-MS

Kumar, K., A.E. Abdulwahab, A. AL-Muftah, V. Alcobia, and A. Carvalho, 2003, Bahrain Field – An Integrated Simulation Study of 15 Reservoirs: Middle East Oil Show, 9-12 June, Bahrain, SPE 81502, 9 p. doi.org/10.2118/81502-MS

Murty, C.R.K., N. Al Saleh, and B.A. Dakessian, 1987, Forty-Seven Years' Gas Injection in a Preferentially Oil-Wet Low-Dip Reservoir: Journal of Petroleum Technology, SPE 13749, v. 39/3, p. 363-368. doi.org/10.2118/13749-PA

Williams, M.A., J.F. Keating, and M.F. Barghouty, 1998, The Stratigraphic Method: A Structural Approach to History Match Complex Simulation Models: SPE Reservoir Evaluation & Engineering, SPE 38014, v. 1/2, 8 p. doi.org/10.2118/38014-PA

Zubari, H.K., and M.Y. Al-Awainati, 1997, Utilizing Well Tests in Determining the Drive Mechanism and Threshold Pressures Between Three Communicating Reservoirs: Middle East Oil Show and Conference, 15-18 March, Bahrain, SPE 37795, 30 p. doi.org/10.2118/37795-MS

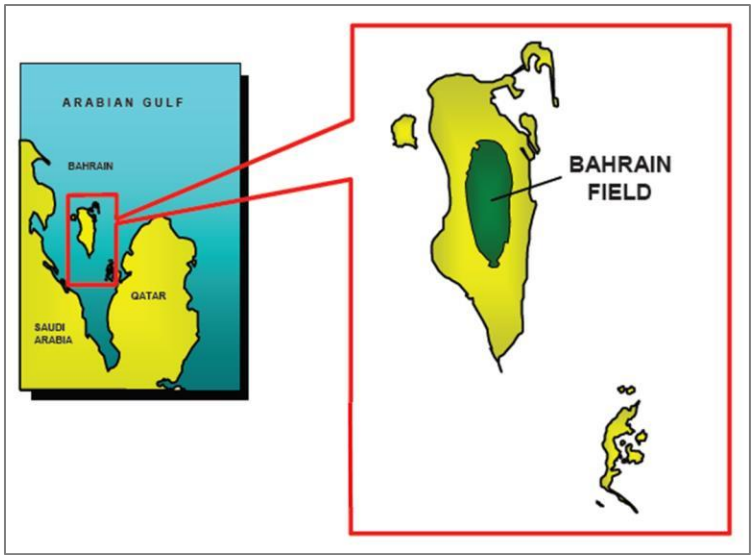

Figure 1. Location of Awali Field, Bahrain.

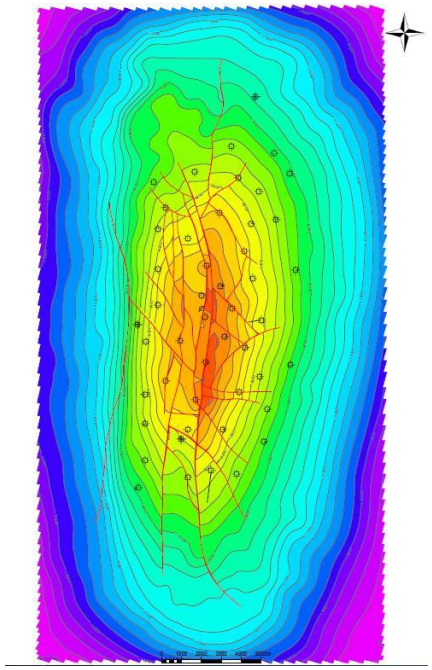

Figure 2. Structure map on top of Khuff reservoir.

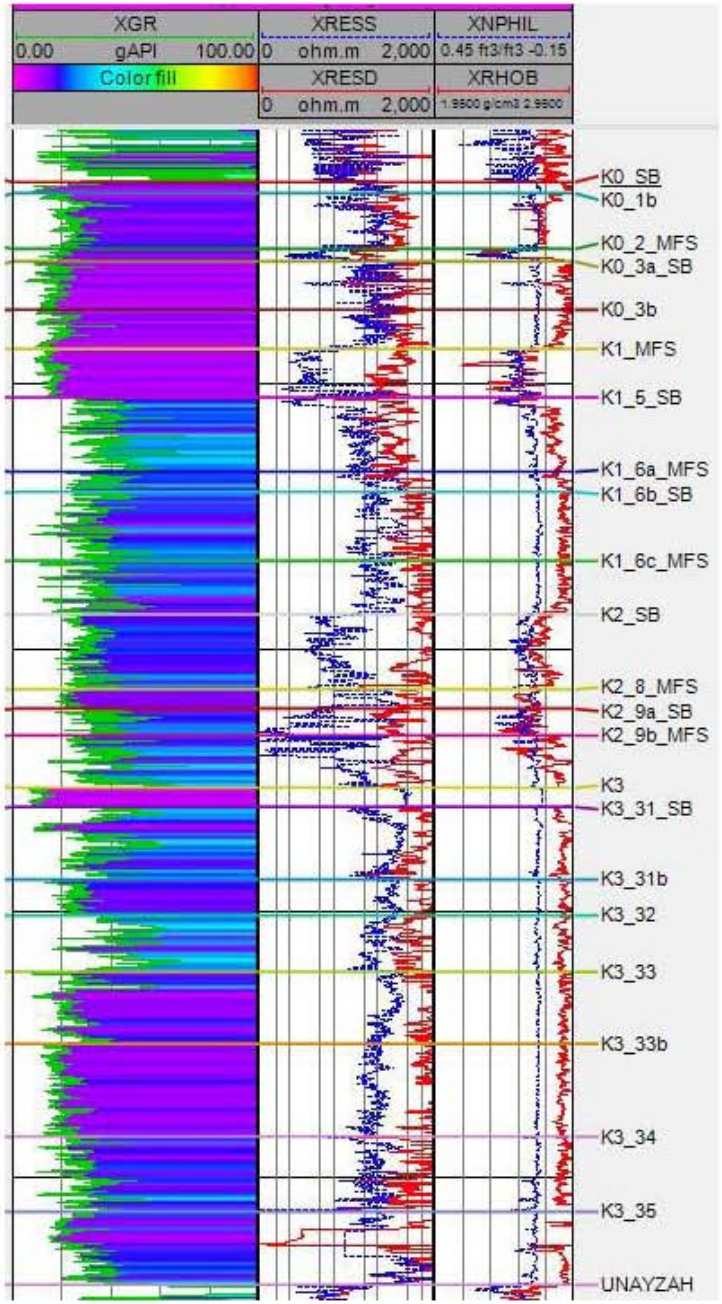

Figure 3. Sequence stratigraphic units in Khuff (SB: Sequence Boundary, MFS: Maximum Flooding Surface).

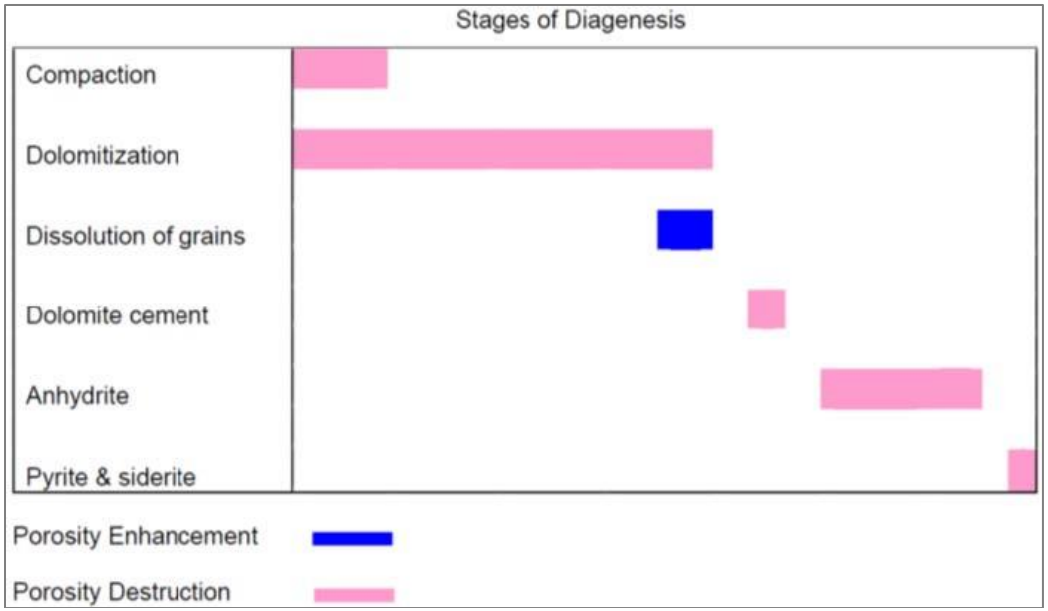

Figure 4. Main diagenetic events identified in Khuff cores.

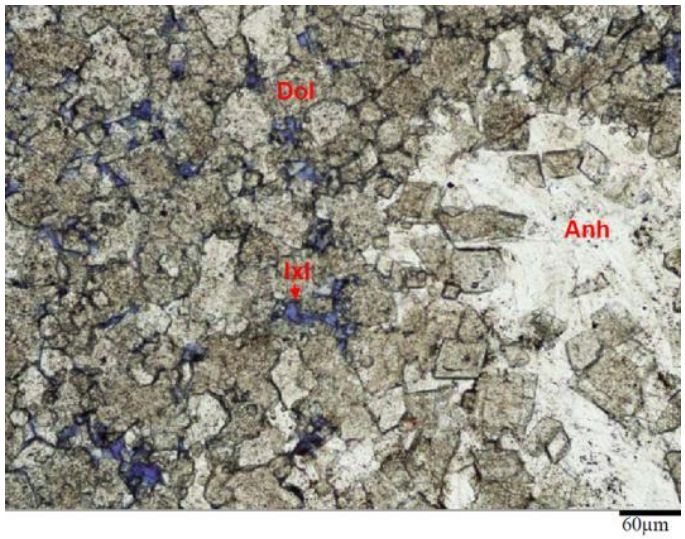

Figure 5. Photomicrograph showing fine to medium crystalline anhedral to euhedral dolomite (Dol). Main porosity type is intercrystalline porosity (Ixl). Anhydrite (Anh) cement present as patchy and occluding the pore spaces.

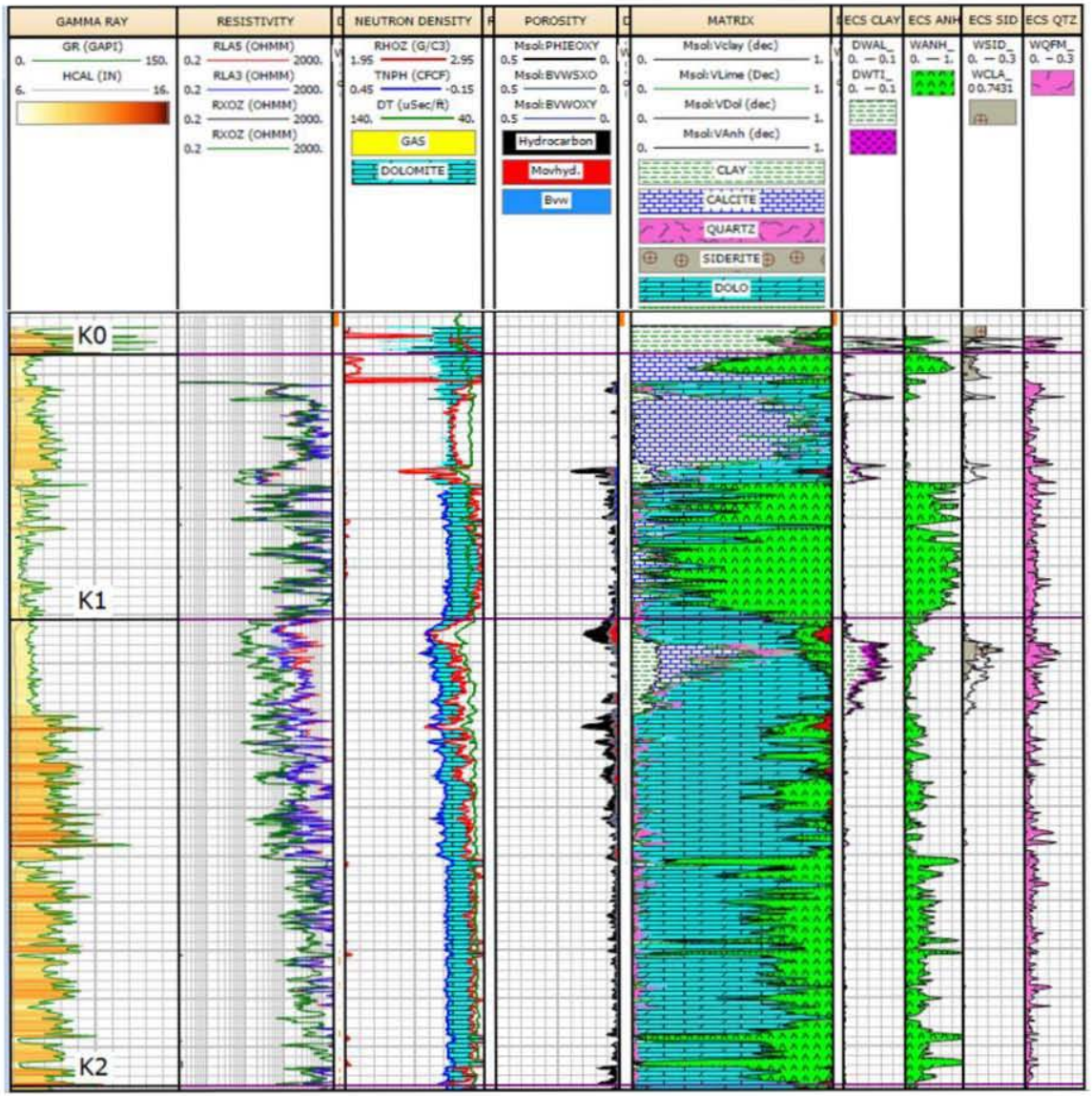

Figure 6. Mineral volume interpretation with ECS data.

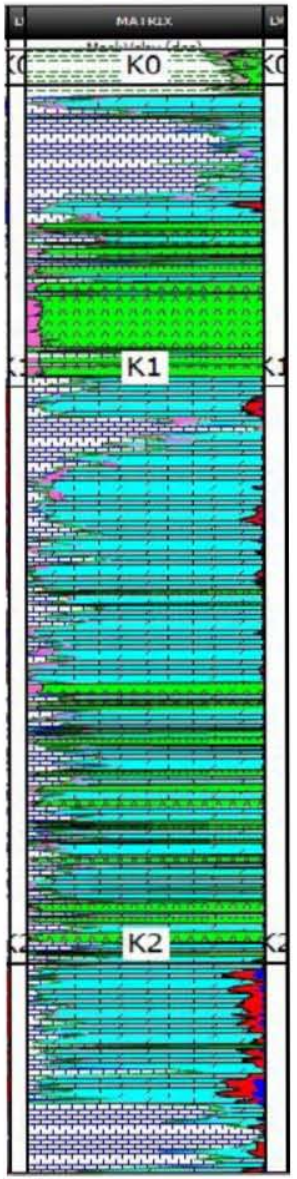

Figure 7. Mineral volume interpretation without ECS data.

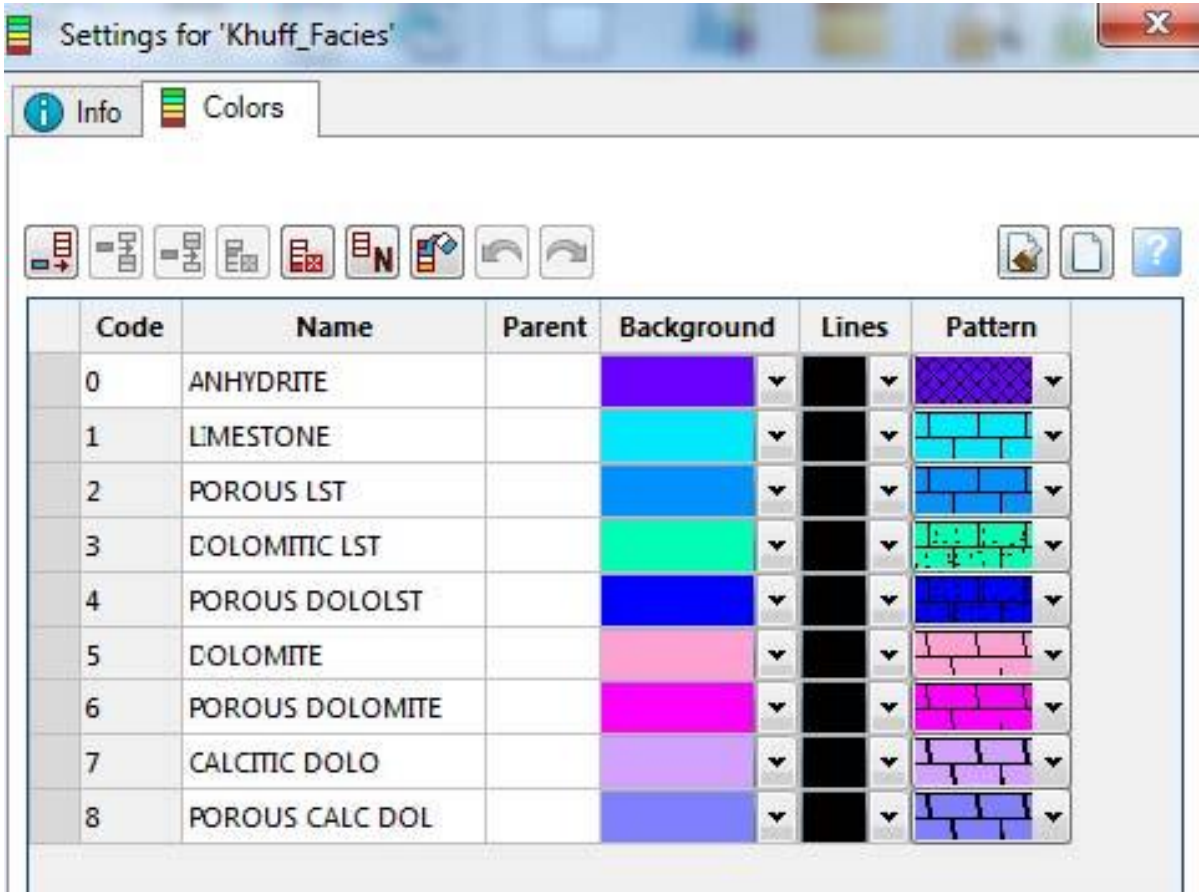

Figure 8. Facies codes for the interpreted Khuff lithofacies.

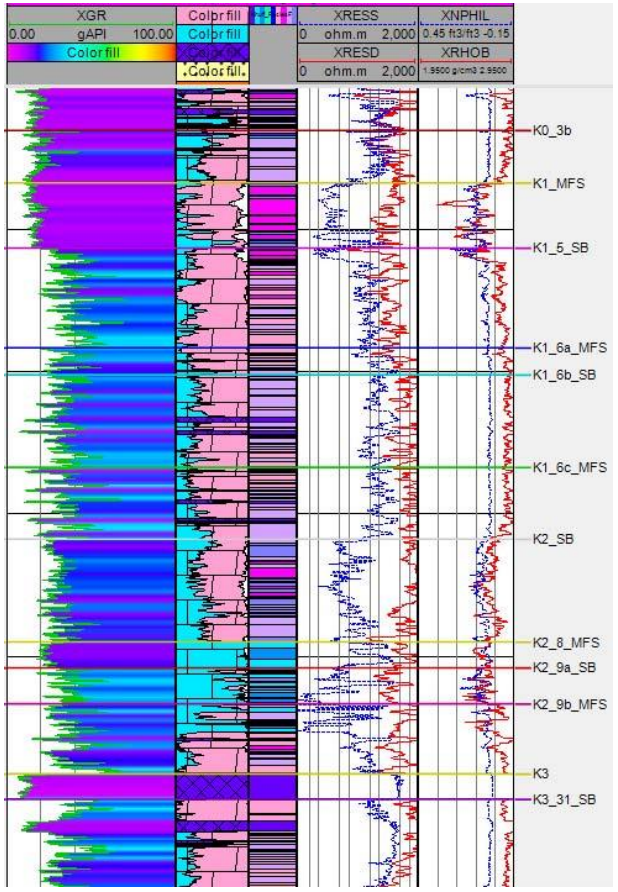

Figure 9. Interpreted facies in Petrel from mineral volume curves.

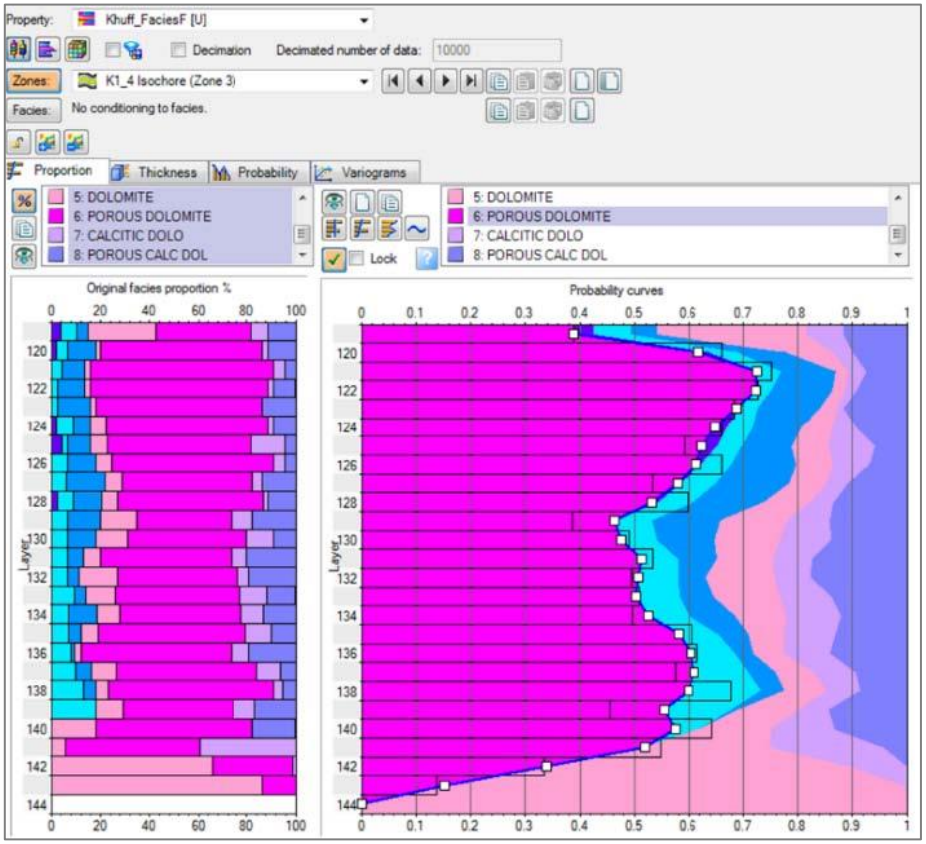

Figure 10. Vertical facies proportion for zone K1_4 (K1_MFS).

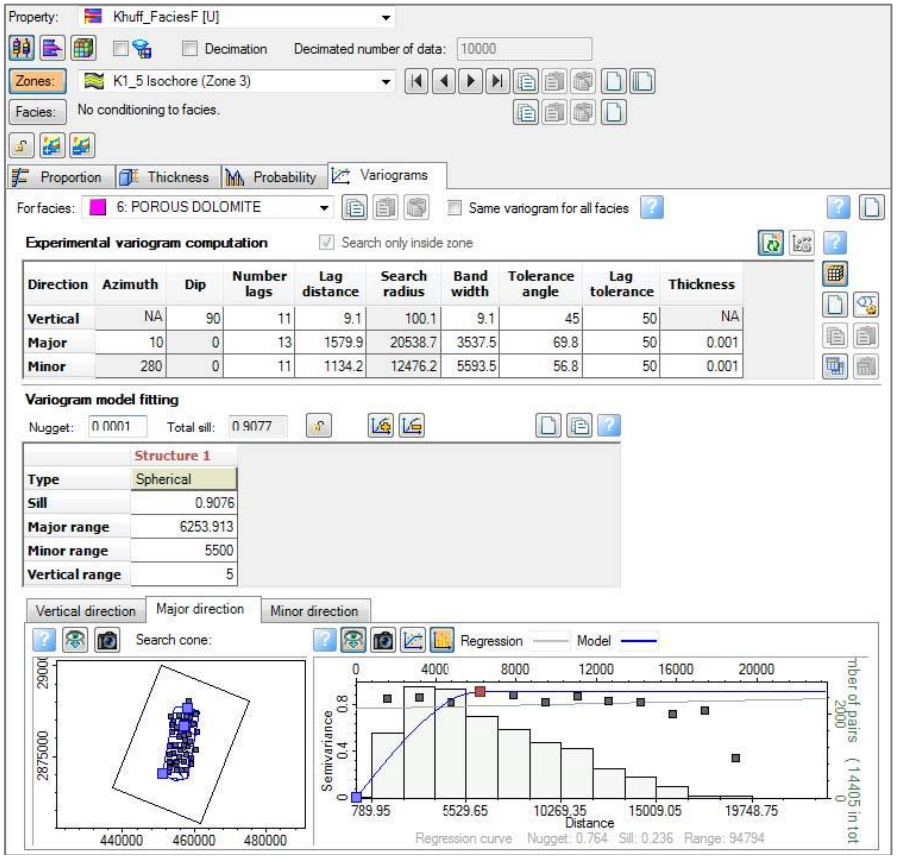

Figure 11. Example of modelled variogram in the Major direction for porous dolomite facies in zone K1_5.

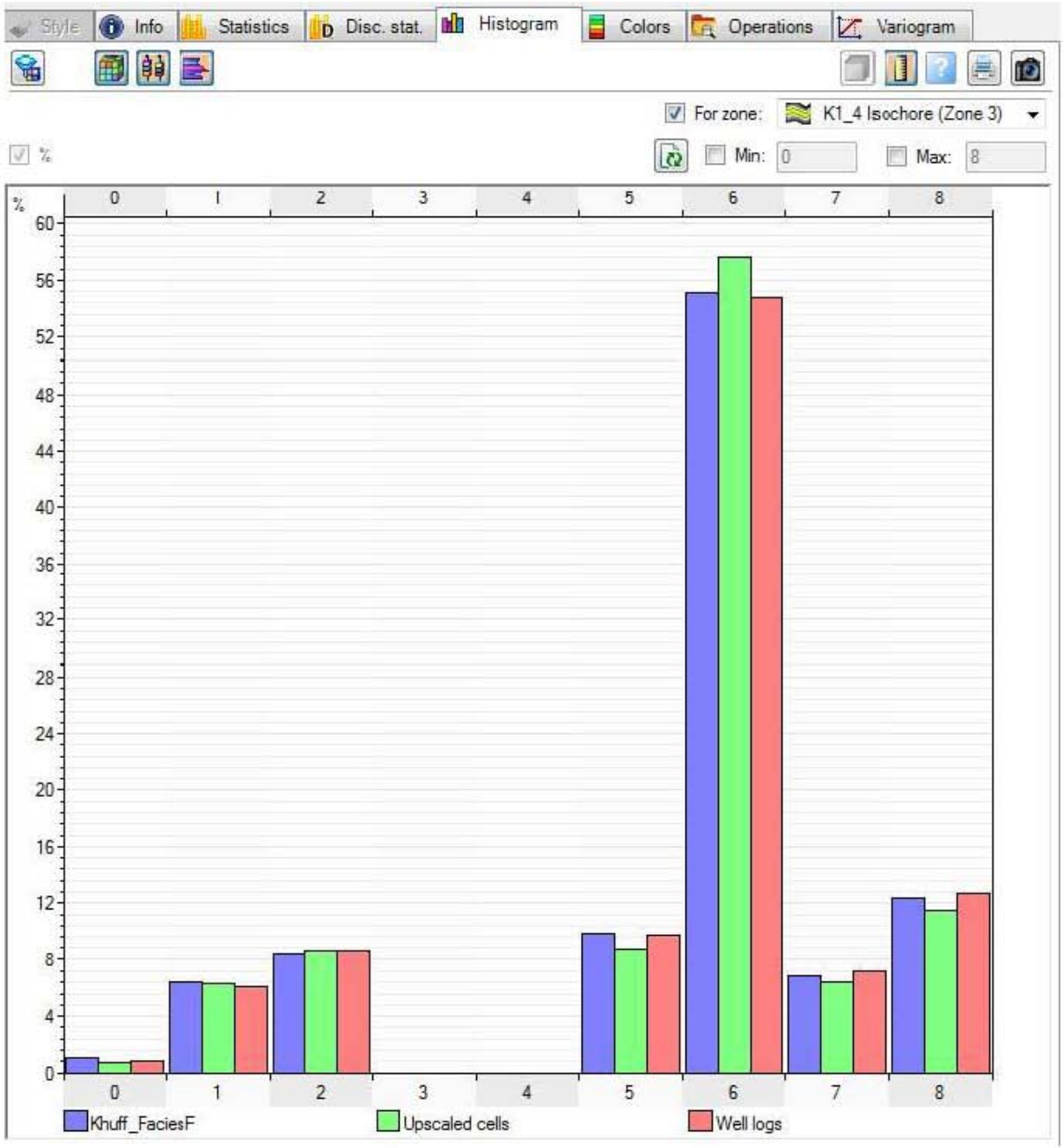

Figure 12. Histogram of modelled vs upscaled and well logs facies showing good match (e.g. zone K1_4).

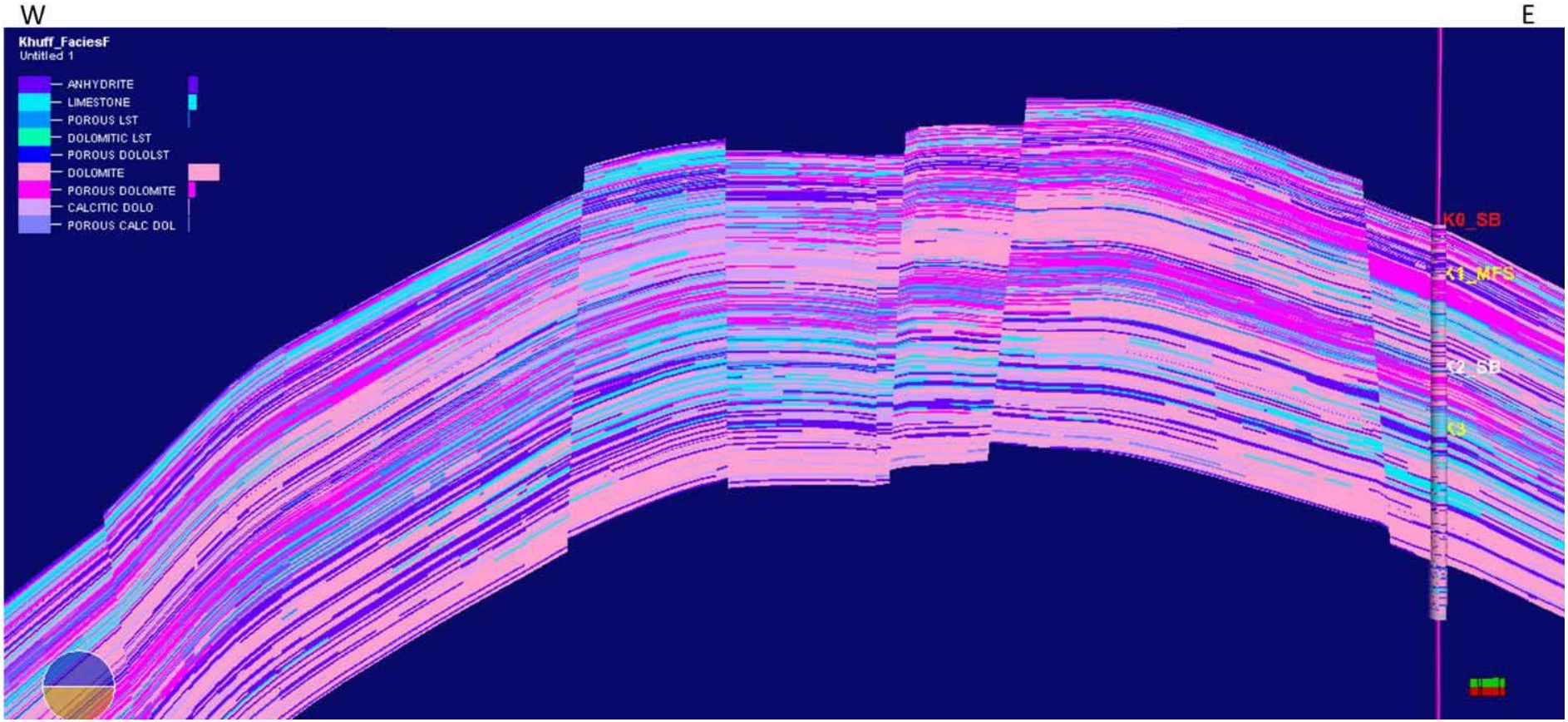

Figure 13. West-East cross section across the Khuff reservoir showing distribution of different lithofacies.

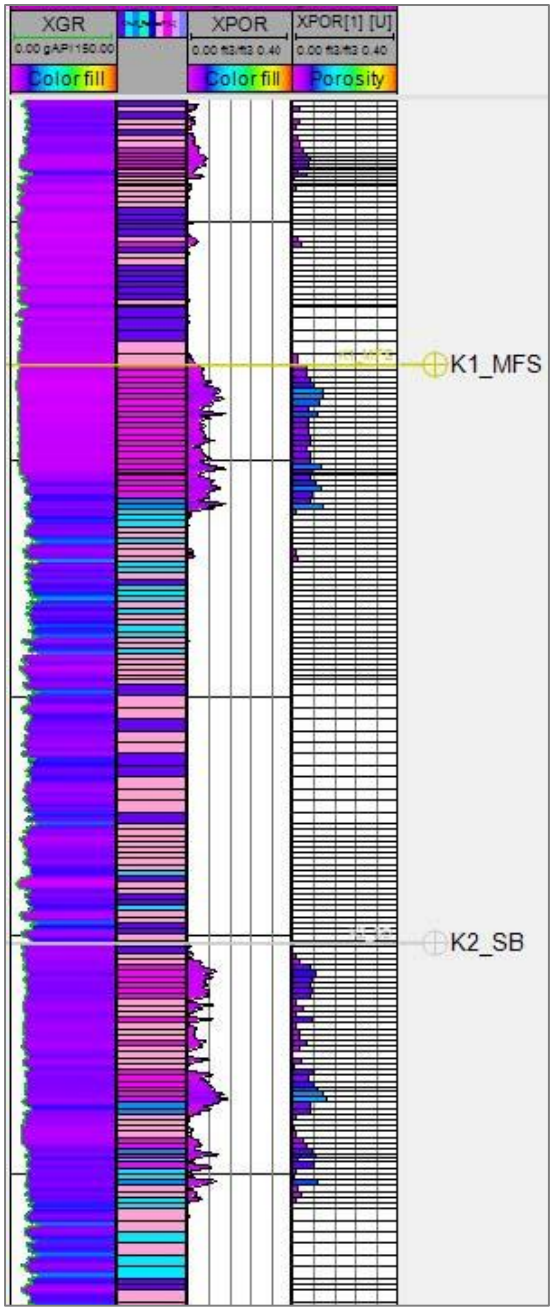

Figure 14. Upscaled porosity log showing good match with input log (Logs from L to R: GR, Upscaled Facies, Porosity, Upscaled Porosity).

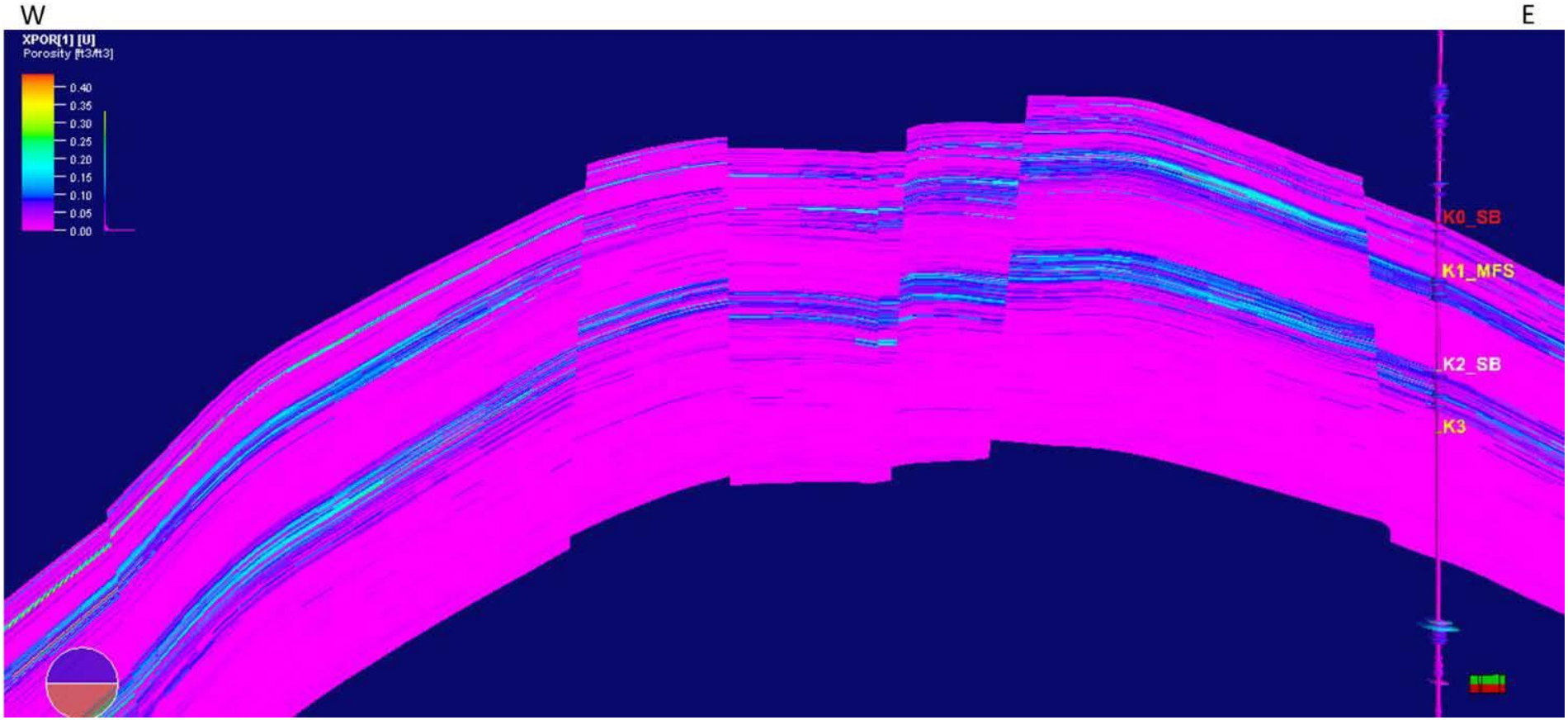

Figure 15. West-East cross section across the Khuff reservoir showing porosity distribution.